Combining *Ab Initio* Techniques with Analytical Potential Functions for Structure Predictions of Large Systems: Method and Application to Crystalline Silica Polymorphs

UWE EICHLER,[1] CHRISTOPH M. KÖLMEL,[2] and JOACHIM SAUER[1]*

[1]*Max Planck Society, Research Unit ''Quantum Chemistry'', Humboldt University, Jägerstr. 10/11, D-10117 Berlin, Germany*

[2]*MSI, 9685 Scranton Road, San Diego, California 92121-3752*

Received 12 February 1996; accepted 18 June 1996

ABSTRACT

A computational scheme is presented which combines quantum mechanical *ab initio* techniques with methods using analytical potential functions. The scheme is designed for use in structure optimizations and is also applicable to molecular dynamics simulations. The implementation covers both molecular and periodic systems. The problem of the link atoms is solved by a subtraction scheme which is easily implemented for any combination of methods. As a first application dense and microporous silica polymorphs are studied. The Hartree–Fock method is combined with both a force field and an ion pair shell model potential. Comparison is made with lattice energy minimizations which use the force field or the shell model potential alone as well as with free cluster optimizations and optimizations in which the outer part of the cluster is kept fixed.

Introduction

In spite of the tremendous progress made with structure predictions by *ab initio* techniques many molecular systems are still too large for a full quantum mechanical treatment. A computationally much more efficient alternative is the use of analytical potential functions ranging from different types of force fields for organic molecules to ion pair type potentials for ionic crystals. However, the success of these techniques is limited by the limited range of applicability of the potential functions available. Force fields yield accurate

* Author to whom all correspondence should be addressed.

CCC 0192-8651 / 97 / 040463-15

structures for organic molecules in regular bonding states, but cannot describe the forming and breaking of chemical bonds. They have also difficulties in describing differently coordinated transition metal sites in organometallic complexes. Force fields and ion pair potentials can also yield accurate bulk structures of solids, but are less suited to describe the structure of active sites of catalysts or of defects in semiconductors and ionic crystals, and they fail completely for reactions involving such sites. The obvious solution to the problem is to partition the large system into the site of interest (the interior part) described by a quantum mechanical method and the environment (the outer part) described by a force field. The assumption is made that the structure of the environment can be modeled accurately by analytical potential functions.

There is a vast[1] and growing[2,3] number of implementations of this idea which focus on different types of systems and which use different quantum chemical methods. Examples are the study of the $CH_3Cl + Cl^-$ reaction in aqueous solution by Singh and Kollman,[4] the test performed by Field et al.[5] for intermolecular interactions, the DFT/AMBER coupling for solvation-free energies by Merz et al.[6,7] and the scheme of Morokuma et al.[3] and Maseras and Morokuma[8] for optimizing structures and transition states of transition metal complexes. Other typical embedding cases are enzymes[9] and heterogeneous catalysts,[10] because embedding schemes are ideally suited to study how the structure and activity of a given active site change when in different environment.

The implementations differ in two important aspects. First, the interaction between the interior part and the environment can include polarization of the electron distribution of the interior part by the electrostatic potential provided by the environment or not. We will refer to these two options as ''electronic'' and ''mechanical'' embedding. Second, there are different ways to treat the boundary region between the interior part and the environment. If the cut can be made such that no chemical bonds between the interior part and the environment are broken there is no special boundary region. A typical case is solvation[1,7] in which whole solvent molecules form the environment for a solute molecule. Other such cases are ionic or molecular crystals where complete ions or molecules form the environment for the site of interest. More difficult to treat are large organic molecules, macromolecules, and solids with covalent or partially covalent bonds. Cutting out the interior part leaves dangling bonds at its border which have to be saturated with hydrogen atoms to create a realistic model for the quantum mechanical description of the interior part.[11] These terminating hydrogen atoms—called link atoms—create specific problems which are solved differently in different implementations.[5,8]

In this article, we present a ''mechanical'' embedding scheme[12] for structure predictions which is designed for periodic environments but can also handle finite molecular systems. It differs from other schemes by special treatment of the link atoms: (i) a subtraction scheme approximately eliminates the contribution of the link atoms to the forces on the nuclei; (ii) the energy is transformed into an expression which explicitly depends on the coordinates of real atoms only, but is an implicit function of the link atom coordinates.

The Methods section of this article describes the present embedding scheme and shows how it compares with others. Then, two implementations[13,14] for periodic systems are presented which differ in type of analytical potential function for the environment. We demonstrate the power of the method by determining the structure of different polymorphs of crystalline silica. Subsequent studies will deal with the effect that the silicate framework has on the structure of Brønsted sites in zeolite catalysts and on their interaction with molecules.

Methods

EMBEDDING SCHEME

We partition the entire system (S), which can be either a molecule of arbitrary size or the unit cell of a periodic system, into the inner region (I) and outer region (O). For simplicity, we first consider the special case that there are no link atoms. The energy of the entire system, $E(S)$, is approximated by the quantum mechanically calculated energy of the inner region, $E_{QM}(I)$, the energy of the outer region calculated from the analytical potential functions, $E_{MM}(O)$, and an interaction term, $E(I-O)$:

$$E(S) = E_{QM}(I) + E_{MM}(O) + E(I-O) \quad (1)$$

There are several options for calculating the interaction term arising from the fact that part of it can

be, but need not be calculated quantum mechanically:

$$E(I-O) = E_{QM}(I-O) + E_{MM-QM}(I-O) \quad (2)$$

$E_{MM-QM}(I-O)$ includes all interaction terms of the analytical potential function which are not covered by the quantum mechanical calculation. $E_{QM}(I-O)$ is frequently the electrostatic interaction of the quantum mechanical charge distribution of the inner region with the point charges belonging to the analytical potential description of the outer region. This is achieved by adding the outer region point charges to the Hamiltonian of the inner region, which accounts also for the polarization of the inner region by its environment.[1] This option is easily implemented into existing quantum mechanical codes and is also part of our implementation.[13] However, the results are not always an improvement over calculations which neglect the point charges of the environment in the Hamiltonian. The reason is that interactions that could counteract a charge polarization, such as electron repulsion and charge penetration, are not included. Even more serious problems can occur when aiming at structure optimizations as we do.

Therefore, calculating the interaction term from the analytical potential function alone and neglecting charge polarization effects turns out to be a more useful approximation:

$$E(I-O) = E_{MM}(I-O) \quad (3)$$

This means that the electrostatic interaction between the two parts is calculated by the point charge interaction term defined in the analytical potential. Hence, we have:

$$E(S) = E_{QM}(I) + E_{MM}(I-O) + E_{MM}(O) \quad (4)$$

While evaluation of $E_{QM}(I)$ requires just a standard calculation for the inner region, $E_{MM}(I-O) + E_{MM}(O)$ is most easily obtained from molecular mechanics calculations for the entire system and for the inner region:

$$E_{MM}(I-O) + E_{MM}(O) = E_{MM}(S) - E_{MM}(I) \quad (5)$$

Hence, our implementation is based on the following equation:

$$E(S) = E_{QM}(I) + E_{MM}(S) - E_{MM}(I) \quad (6)$$

The difference, $E_{MM}(S) - E_{MM}(I)$, is evaluated numerically while most other implementations get it by removing all terms from the expression for $E_{MM}(S)$, which are assumed to be covered by $E_{QM}(I)$. This requires modifications on the MM code whereas application of eq. (6) does not.

The advantage of our scheme becomes obvious when we consider systems that require link atoms to terminate the dangling bonds created by cutting out the inner region. The system on which the quantum mechanical calculations are performed is called the cluster (C) and is composed of the inner region and the link region (L). The energy of the entire system is approximated as follows:

$$E(S) = E_{QM}(C) + E_{MM}(O) + E_{MM}(I-O) - E_{QM}(L) - E_{QM}(I-L) \quad (7)$$

The last two terms reflect that the link atoms are not part of the system to be described and that energy contributions connected with them have to be removed. The molecular mechanics energy of the entire system can be broken down similarly:

$$E_{MM}(S) = E_{MM}(C) + E_{MM}(O) + E_{MM}(I-O) - E_{MM}(L) - E_{MM}(I-L) \quad (8)$$

Substituting $E_{MM}(I-O) + E_{MM}(O)$, obtained from this equation, into eq. (7), yields:

$$E(S) = E_{QM}(C) + E_{MM}(S) - E_{MM}(C) + \Delta \quad (9)$$

with:

$$\Delta = E_{MM}(L) - E_{QM}(L) + E_{MM}(I-L) - E_{QM}(I-L) \quad (10)$$

If our analytical potential function mimics the quantum mechanical energy contributions connected with the link region sufficiently well, Δ can be neglected and the influence of the link atoms is removed. There is no way to remove $E_{QM}(L) + E_{QM}(I-L)$ directly from the quantum mechanical energy of the cluster.

With $\Delta = 0$, our final energy expression is:

$$E(S) = E_{QM}(C) + E_{MM}(S) - E_{MM}(C) \quad (11)$$

If there are no link atoms C is equal to I; i.e., eq. (6) is a special case of the above equation.

The forces on the nuclei, which are needed for the structure optimizations, are given by an analogous relation:

$$F_\alpha(S) = F_{\alpha,QM}(C) + F_{\alpha,MM}(S) - F_{\alpha,MM}(C) \,\big|\, \alpha \in I \tag{12a}$$

$$F_\beta(S) = F_{\beta,MM}(S) \,\big|\, \beta \in O \tag{12b}$$

For an atom α of the inner region, all three terms contribute to the force on the atom. For an atom β of the outer region, the force is obtained from the molecular mechanics expression alone. A link atom is not moved according to the force acting on it. It is instead kept fixed on the bond which it terminates. Details are given in the next section.

In case of a periodic system, a completely analogous relationship exists for the forces on the unit cell. The strain derivatives, $F_{mn}(S)$, are given by:

$$F_{mn}(S) = F_{mn,QM}(C) + F_{mn,MM}(S) - F_{mn,MM}(C) \tag{13}$$

Here, the contribution of the finite cluster to the strain derivatives is computed by the general expression ($X = QM$ or MM)

$$F_{mn,X}(C) = \sum_{\alpha}^{I} r_{\alpha,m} \frac{\partial E_X(C)}{\partial r_{\alpha,n}} \tag{14}$$

where the sum runs over all atoms, α, of the inner region.

The absolute energies of analytical potential functions, in contrast to the relative energies, are without physical significance. In taking energy derivatives, any arbitrary additive constant disappears, and the three forces in eq. (12a) are all directly comparable. This is not valid for the energies, for which two different constants appear, one for the cluster and the other for the host. From this follows that total energies are only comparable if clusters of the same size are used and if the same system is considered.

The scheme outlined above has general applicability. It can be used, in principle, to combine any pair of methods capable of computing the potential energy for the inner and outer regions. This means that, for example, the QM method can be a semiempirical, an *ab initio* or a density functional method. It could as well be applied to cases in which a high-level QM method is combined with a low-level QM method. The only requirement is that Δ [eq. (10)] approaches zero, which may not be the case for all formally possible combinations of methods. Eq. (10) also shows that combinations which strive for consistency between the quantum mechanical method used for the cluster and the potential functions used for the environment are particularly promising. Potential functions which are parameterized on the basis of *ab initio* data rather than on the basis of empirical data appear particular attractive, because the *ab initio* data can be generated using the same quantum mechanical approximation as used for the treatment of the cluster. This is the approach we adopt in the applications that follow.

SPECIAL TREATMENT OF LINK ATOMS

A link atom is used to terminate a dangling bond created when cutting out the inner region from a system. If there was a bond between atom A of the inner region, say, and atom B of the outer region, a link atom H is introduced to replace atom B resulting in an A—H bond. The link atom lies on the original A—B bond axis, while the A—H bond distance is kept fixed. The value of this distance can best be determined by free space optimizations of the cluster model, as done in this work. Because the coordinates of the link atoms are completely determined by the coordinates of the other atoms in the system, it is possible to transform the energy expression, and thus the energy gradient, to not explicitly depend on link atom coordinates. This means that, in a structure optimization, only the ''real'' atoms have to be dealt with.

The total energy calculated for the system is a function of the coordinates of the ''real'' atoms of both the inner and outer regions (subscript X) and any link atoms (subscript H) that have been introduced:

$$E = E(\mathbf{r}_X, \mathbf{r}_H) \tag{15}$$

Because the link atom positions are a function of the coordinates of the ''real'' atoms, $\mathbf{r}_H = \mathbf{r}_H(\mathbf{r}_X)$, the energy depends explicitly only on the position of the real atoms:

$$E = E(\mathbf{r}_X, \mathbf{r}_H(\mathbf{r}_X)) = \tilde{E}(\mathbf{r}_X) \tag{16}$$

If the energy is differentiated with respect to the coordinates of a real atom, X, the chain rule has to be applied:

$$\frac{d\tilde{E}}{dr_{Xm}} = \frac{\partial E}{\partial r_{Xm}} + \sum_{i=1}^{3} \frac{\partial E}{\partial r_{Hi}} \frac{\partial r_{Hi}}{\partial r_{Xm}} \tag{17}$$

If the link atom H is fixed on the bond axis $A-B$ at a distance r_{AH} from atom A, its position is given by:

$$\mathbf{r}_H = \mathbf{r}_A + g(\mathbf{r}_B - \mathbf{r}_A) \tag{18}$$

with $g = r_{AH}/r_{AB}$. Differentiation of the vector components of the position of the H atom with respect to the components of the positions of the and B atoms yields:

$$\frac{\partial r_{H,m}}{\partial r_{B,n}} = -g n_m n_n + g\delta_{m,n} \tag{19}$$

$$\frac{\partial r_{H,m}}{\partial r_{A,n}} = \delta_{m,n} + g n_m n_n - g\delta_{m,n} \tag{20}$$

The indices m and n denote the Cartesian components, x, y, z, of the respective vectors. δ is the Kronecker symbol. $\mathbf{n}$ is the unit vector parallel to the $A-B$ axis and pointing toward B. If these equations are then inserted into eq. (17) the following relations are obtained:

$$\frac{d\tilde{E}}{dr_{B,m}} = \frac{\partial E}{\partial r_{B,m}} - g\left[\frac{\partial E}{\partial \mathbf{r}_H}, \mathbf{n}\right] n_m + g\frac{\partial E}{\partial r_{H,m}} \tag{21}$$

$$\frac{d\tilde{E}}{dr_{A,m}} = \frac{\partial E}{\partial r_{A,m}} + g\left[\frac{\partial E}{\partial \mathbf{r}_H}, \mathbf{n}\right] n_m + (1-g)\frac{\partial E}{\partial r_{H,m}} \tag{22}$$

The entities in square brackets are scalar products. The derivatives of the energy with respect to the link atom coordinates, $\partial E/\partial \mathbf{r}_H$, generally do not completely vanish applying the subtraction scheme defined by eq. (13). They would vanish only if both the QM and MM methods would yield exactly the same potential. If the unit cell dimensions are to be optimized as well, only the derivatives, $\partial \tilde{E}/\partial \mathbf{r}_\alpha$ ($\alpha \in I$), are taken into account when computing the contribution of the cluster to the cell derivatives.

This scheme differs from published schemes which either ignore the influence of the link atoms and let them move freely during optimization[5] or apply the constraint of constant bond length to the A—B and A—H bond.[8] In this work, we do impose an optimization constraint, but on the artificially introduced link atoms, instead of on any real atoms.

POTENTIAL FUNCTIONS USED

We consider two types of analytical potential functions, force fields for dominantly covalent systems and ion pair potentials for ionic or partially ionic crystals.

Most current force fields are composed of two major contributions. The first contribution includes so-called bond terms, which describe interactions between atoms that are separated by up to three chemical bonds. These interactions are usually cast into the functional form of a generalized valence force field, which depends on bond lengths, bond angles, and torsion/dihedral angles, and couplings between them. For the bond distance and angle terms a Taylor series expansion about the respective equilibrium values is used, which can lead to difficulties for systems having bond distances or bond angles that can vary over a broad range (see, e.g., Hill and Sauer[15] for such a case with relevance to the present application). The second contribution are the so-called nonbond terms. They cover interactions derived from first- and second-order intermolecular perturbation theory; i.e., (exchange) repulsion, electrostatic interactions, and dispersion forces. There are many different versions of force fields in use, most of them come in combination with the different structure optimization and simulation codes. While previous embedding studies used AMBER,[16] CHARMM,[17] or MM2,[18] our implementation employs the CVFF[19] and CFF91[20] force fields which are available in the DISCOVER simulation code.[21] Ion pair potentials are widely used for modeling inorganic materials. They are particularly successful when combined with the shell model proposed by Dick and Overhauser,[22] which accounts for polarization effects. The shell model represents an ion, e.g., the O^{2-} ion in silica, by a pair of point charges, the positive core and the massless negative shell, which are connected by a harmonic spring. The electrostatic energy is evaluated for all cores and shells and the shell positions are optimized to yield the lowest energy. Nonbond repulsion and attraction terms are added, mostly between equally charged ions. Such potentials are typically used in codes that perform lattice energy minimizations for periodic systems.[23]

IMPLEMENTATION

The first implementation of the present embedding scheme is realized in the program SOLIDS_EMBED,[13] which allows to combine the *ab initio* program TURBOMOLE,[24] the density functional program DMol[25] or the semiempirical program MOPAC[26] with the force field code DIS-

COVER.[21] It includes the option to treat the inner part–outer part coupling quantum mechanically, i.e., to account for the polarization of the inner part electron distribution by the electrostatic potential of the outer part.

The second implementation of the presented embedding scheme[14] combines the *ab initio* code TURBOMOLE[24] with the shell model potential for the environment of the cluster. The shell model calculations are carried out with the GULP program.[23] The use of the shell model requires two additional steps, namely the optimization of the shells of the cluster and the host while the cores are fixed. For the configurations with the converged shell positions the energy gradients are calculated for the cores and then combined with the energy gradients resulting from the SCF calculation.

In both implementations, the resulting combined energy gradient with dimension $3n$, where n is the number of host atoms, is then used by a BFGS quasi-Newton optimizer which updates the structure for the next cycle until convergence is reached as measured by the change of the total energy. Figure 1 shows the implementation.

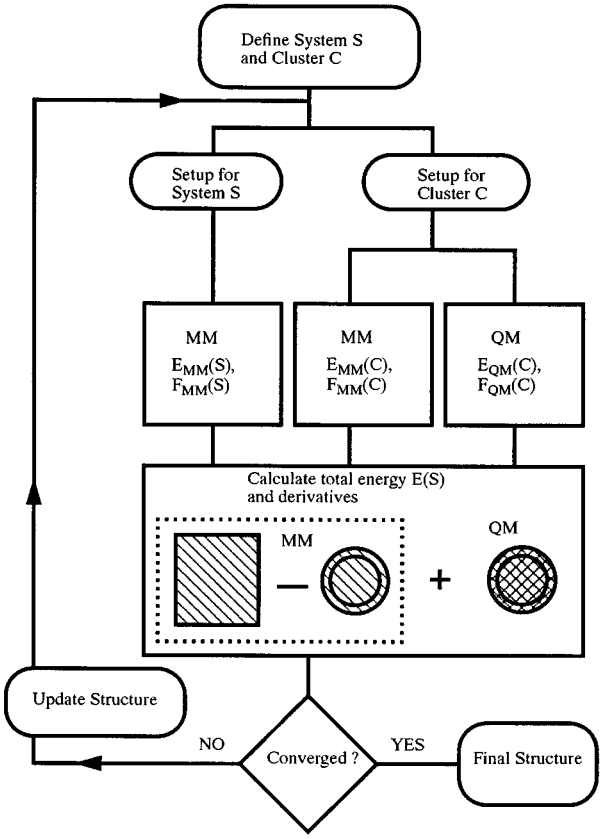

FIGURE 1. Flow chart of the implementation of the embedding scheme.

Structure Predictions for Crystalline Silica Polymorphs

INTRODUCTION

Crystalline silica polymorphs do not merely play a key role in many applications, because of their structural richness they are also attractive systems for testing methods. The dense polymorph, quartz, is a well-characterized system which is frequently studied by theoretical methods. The microporous polymorphs, sodalite and faujasite, are of interest as all-silica end-members of series of zeolite catalysts with decreasing Al content. For all three polymorphs, structure information is available from diffraction and from solid-state MAS-NMR experiments. Moreover, for quartz and sodalite, periodic quantum mechanical calculations are feasible at the Hartree–Fock (HF) level.[27] For the quantum mechanical description of the cluster we use the HF method with a polarized basis set which is a standard approximation for structure determination. For faujasite we use two types of analytical potential functions to embed the cluster, a force field type potential,[15] and a shell model ion pair potential.[28]. The shell model potential was employed for all three polymorphs, because it gives better results for the lattice energy minimization than the force field. To study the influence of the cluster size, the cluster dimensions were systematically increased. The validity of the results was evaluated by comparisons with experimental values and results from periodic HF calculations. The structures obtained by the embedding calculations were also compared with structures obtained by cluster optimizations in which, on the one hand, all degrees of freedom were relaxed and, on the other hand, the terminating hydroxyl groups were kept fixed.

DETAILS OF QUANTUM MECHANICAL CALCULATIONS FOR THE CLUSTER

The energy and energy gradient calculations for the cluster were done in the HF approximation using the program TURBOMOLE.[24] For silicon and hydrogen, basis sets of double-zeta plus polarization (DZP) quality were used. For the oxygen atoms, a triple-zeta plus polarization (TZP) basis set has been applied.[29] For the Si/O/H atoms, the

(11*s*,7*p*)/(9*s*,5*p*)/(4*s*) Gaussian basis sets were taken from Huzinaga[30,31] contracted into the following pattern {5 2 1 1 1 1, 4 1 1 1}/{5 1 1 1 1, 3 1 1}/{3 1}. Polarization functions with the following exponents were added: 0.4 (Si), 1.2 (O), and 0.8 (H). This basis set, denoted as DZP/TZP(O), is exactly the same as the one used for establishing the quantum chemical data to which the potentials were fit. The cutout was made such that the clusters terminate with OH groups. The fixed link atom distance, r_{OH}, was set to 94.5 pm throughout. This value was obtained by free cluster optimizations with the same basis set.[32] All SCF calculations were carried out in C_1-symmetry. The free and restricted cluster optimizations were performed with the same basis set. The fixed coordinates of the terminating hydroxyl groups were taken from an initial lattice energy minimization with the same potential as used in the embedding calculation. The inner parts of these clusters were relaxed until the largest Cartesian gradient component of the relaxed atoms was lower than 0.001 Hartree/Bohr.

POTENTIALS USED TO EMBED THE CLUSTER

Ab Initio Parameterized Potential Function

An important aspect of this application is the use of analytical potential functions which have been parameterized on *ab initio* data obtained at the same level of approximation as employed for the quantum mechanical calculation on the cluster. Such a data base for silica and zeolites has been generated by Hill and Sauer[15,32] and used to parameterize both a ''consistent force field potential''[15,32] and a shell model ion pair potential.[28] Thus, these two potentials differ only in their functional form, but cover the same range of data. This approach has the significant advantage of consistency between the quantum mechanical method applied to the cluster and the potential functions applied to the environment. In particular, this choice of potential function makes it very likely that the effect of the link atoms cancels [$\Delta \approx 0$, cf. eq. (10)]. For the shell model potential it is in fact unavoidable to use *ab initio* data for the fitting, because our scheme also requires shell model calculations on the clusters which are saturated with H atoms. Empirically parameterized shell model potentials cannot provide parameters for these terminating H atoms which are missing in the real solid.

As far as the ''consistent force field'' for silicates and zeolites is concerned it turned out that for embedding calculations the parameters for the saturating hydrogen atoms have to be modified. The reason is that the Si—O—H angles in embedding calculations attain the same range of values as the Si—O—Si angles in the solid. This range (140° to 180°) is very different from the equilibrium values of the Si—O—H angles for free space models (about 115°) around which the structures in the data base cluster. Therefore, the Si—O—H angle parameters had to be refitted using a modified data base.

Modified Consistent Force Field for Silica

For the refit of the link atom parameters a trisilicic acid model was used, $(HO)_3SiO\,Si(OH)_2OSi(OH)_3$. The distorted structures were generated by distortions in internal coordinates. The O—H bond distance was varied within a range of 82 pm to 106 pm. The range of Si—O—H angles chosen was from 116° to 180°. The lower angles were included to make sure that the reference value of that coordinate appeared in the data set. The internal coordinates were varied both separately and simultaneously for proper fitting of the coupling parameters. The SCF energy and gradients were calculated for a total of 44 configurations using the TURBOMOLE program.[24] A split valence plus polarization basis set[33] was chosen because it yields equilibrium structures comparable to those obtained with the DZP/TZP(O) basis set used for establishing the data base for the original potential. As a further modification of that force field the number of atom types was reduced. An oxygen atom which is bonded to silicon and hydrogen has the same atom type as one which is connected to two silicon atoms; that is, the atom types ''oss'' and ''osh'' of the original force field[15] are merged into a single atom type ''os.'' This leads to a decrease of the number of parameters and less computational costs for establishing the data base. The van der Waals parameters of the new atom type ''os'' were taken from the atom type ''oss.'' The charges in this potential are evaluated by bond increments and are therefore different if atoms with the same atom type are bonded to different partners. The parameters of the atom type ''os'' not belonging to the hydrogen atoms are then identical with those of atom type ''oss'' of the original force field. This means that lattice energy minimizations which use this modified force field will yield the same energies and structures as the

TABLE I.
H-Parameters of the Modified Consistent Force Field.[a]

Force field terms	Force field parameters	Unit
Bond: os—hos	$r_0 = 0.9378$; $K_2 = 595.1191$; $K_3 = -1898.1757$; $K_4 = 7195.6401$	r_0 [Å]; K_n [kcal/(mol · Å^n)]
Angle: hos—os—si	$\theta_0 = 120.8765$; $H_2 = 19.5270$; $H_3 = -10.7854$; $H_4 = -0.3450$	θ_0 [deg]; H_n [kcal/(mol · rad^n)]
Torsion: hos—os—si—os	$V_1 = 1.5183$; $V_2 = 1.3782$; $V_3 = 0.0590$	V_n [kcal/mol]
Bond/bond: hos—os—si	$F_{bb'} = -75.0184$	kcal/(mol · Å^2)
Bond/angle: hos—os—si	$F_{b\theta} = 15.6697$; $F_{b'\theta} = 17.7755$	kcal/(mol · Å · rad)
Angle/angle/torsion: hos—os—si—os	$K_{\theta\theta'\phi} = 2.9339$	kcal/(mol · rad^2)

[a] All other parameters are the same as those given in ref. 15.

original force field for hydrogen-free silica polymorphs. Therefore, no explicit tests for the quality of the force field alone were necessary. The modified hydrogen parameters are listed in Table I.

EMBEDDED CLUSTER STRUCTURE DETERMINATION

The start structures for the total energy minimization were created by lattice energy minimizations with the same potential (force field or shell model) as used for embedding. This has the advantage that the structures for the embedding calculations are already nearly converged for the part of the system which is described by the potential only. This initial optimization is also used to determine the cell parameters when they are fixed in the embedding calculation (shell model potential). The embedding calculations are carried out without assuming any symmetry. The P1 spacegroup is also used if the solid is of higher symmetry since the embedding of a cluster destroys the symmetry. In the case of the force field constant pressure minimizations are performed. The shell model potential optimizations were done with constant volume. The size of the unit cell is chosen such that the clusters of different cells do not overlap. As convergence criterion an energy threshold of 1 J/mol was taken. This very tight criterion is a consequence of the very shallow Si—O—Si bending potential.

RESULTS

The smallest model which includes the typical Si—O—Si building unit of silica structures and which is saturated by OH groups is the disilicic acid molecule, $(HO)_3Si—O—Si(OH)_3$. Because it represents two SiO_4 tetrahedra of the silica network, it may also be written as [T, T]. Figure 2 sketches the definition of the inner and outer region as well as the link atom region for this model. A free-space optimization of its structure (constraint to C_s symmetry to avoid formation of internal hydrogen bonds) yields bond distances and angles which are close to the average values found for silica, but do not reflect any structure specificity of the different polymorphs.

All-Silica Faujasite

Faujasite is a zeolite with only one unique tetrahedral (T) site, which is occupied by a silicon atom. This T site is tetrahedrally coordinated by four crystallographically distinct oxygen atoms. This offers four different possibilities to embed the

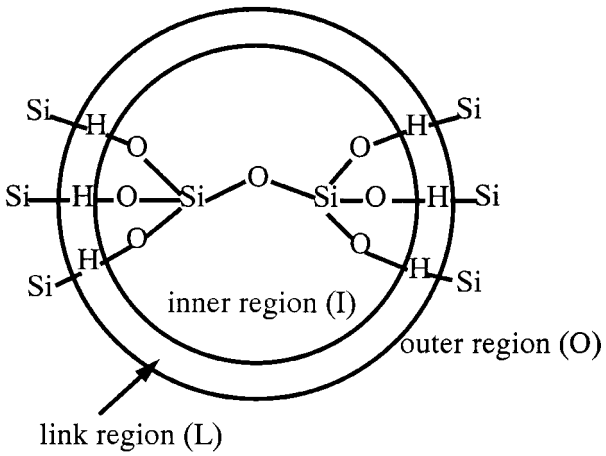

FIGURE 2. Definition of a di-tetrahedra cluster for a silica structure.

TABLE II.
Faujasite Structures Obtained for Di-Tetrahedra $(OH)_3SiOSi(OH)_3$ Models Embedded Using a Consistent Force Field.

O sites	O1	O2	O3	O4	Unit cell parameters
Cluster 1	**1.622**	1.598	1.608	1.608	17.50, 17.50, 17.50
	132.2	167.2	163.2	144.0	60.0, 60.0, 60.0
Cluster 2	1.626	**1.607**	1.609	1.606	17.49, 17.49, 17.50
	133.8	**161.5**	162.6	144.2	60.0, 60.0, 60.0
Cluster 3	1.627	1.596	**1.612**	1.606	17.45, 17.51, 17.51
	131.9	165.6	**157.2**	145.7	60.0, 60.1, 60.1
Cluster 4	1.630	1.600	1.603	**1.612**	17.47, 17.50, 17.50
	131.8	165.4	163.5	**143.4**	60.0, 60.1, 60.0
Potential[a]	1.633	1.623	1.628	1.626	17.56
	135.0	164.6	161.9	144.8	60.0

Upper row, Si—O bond distances, in angstroms; lower row Si—O—Si bond angles, in degrees.
[a] Ref. 15.

di-tetrahedra model [T, T] into the periodic structure. Each of the four crystallographically distinct O atoms can be chosen as O atom of the central Si—O—Si unit (see Fig. 3). All four embedded clusters were used for structure predictions. Table II shows the bond distances and angles obtained with the embedded cluster calculations using the force field potential. In contrast to the embedding calculations with the shell model potential (*vide infra*), the unit cell parameters were optimized simultaneously with the fractional coordinates. For comparison, the structures obtained by lattice energy minimization employing the same potential and the neutron diffraction results (Table III)[34] are also given. The calculated values are given in the following format: The diagonal blocks contain the results for the central Si—O—Si unit of the given cluster (printed in bold) which are the most relevant ones when comparing with the experiment. However, the models contain six additional O atoms which belong to the bordering Si—O—H groups of the embedded cluster and which are of a different crystallographic type. If the embedding method worked perfectly, there would be no difference between the results for a O(n) site found in a central Si—O(n)—Si unit or in a peripheral Si—O(n)—H unit of another cluster. Hence, comparing the results of the different blocks within one column of the table [i.e., comparing the results obtained for a particular O(n) site adopting different clusters] allows internal tests of how well the embedding scheme works.

The most important conclusion is that embedding into the periodic structure leads to four different structure for the embedded di-tetrahedra model. Moreover, the characteristic pattern of the four different Si—O—Si bond angles is nicely reproduced, although deviations from the observed structure may be as large as 10°. We should keep in mind, however, that the potential for

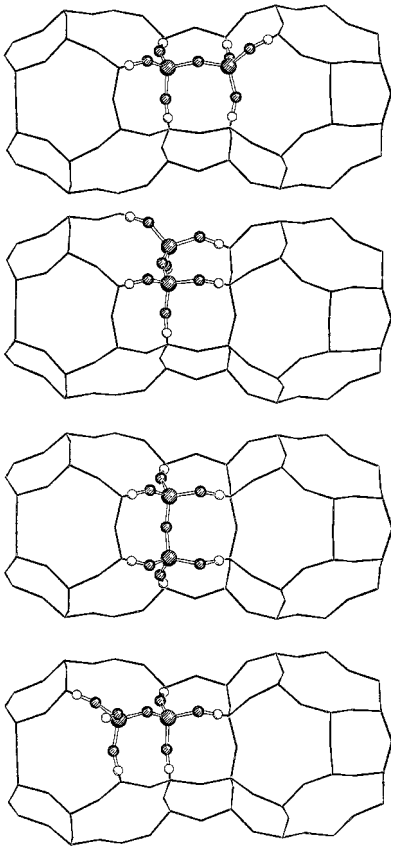

FIGURE 3. Di-tetrahedra models used for faujasite. From top to bottom: O1, O2, O3, and O4 positions.

changing the Si—O—Si angle is extremely low and that small energy changes can cause relatively large bond angle distortions. The predicted bond distances deviate by 0.015 Å or less from the observed values, which is well within the expected accuracy limit of a HF structure prediction. The consistency check of the results within one column of the table yields very rewarding results. The largest deviations found are about 0.1 Å and 6° for the bond distances and bond angles, respectively (positions O2 and O3). A similar crosscheck can be made for the energy. Because all clusters are of the same size, the calculated energies for all four embedded clusters should be the same if the errors of the potential calculations are the same for these four calculations. In practice, four different energies are obtained. If the energy for cluster 4 is set to zero, the relative energies for clusters 1, 2, and 3 are −4.1, −3.5, and 13.0 kJ/mol. The calculated energies are therefore accurate only to about 20 kJ/mol.

The results for embedding the same four clusters into an environment described by the shell model ion pair potential are shown in Table III. The accuracy of the energies as estimated from a comparison of the results for the four different clusters is better than 10 kJ/mol. The relative energies for clusters 1, 2, and 3 with respect to cluster 4 are 0.2, 6.2, and 4.4 kJ/mol; that is, compared to embedding by the force field the accuracy is improved by a factor of two. That the minimized structures are of higher accuracy than those obtained by the force field potential is also obvious from the absolute values of the bond angles. The superiority of the shell model potential is already seen from the lattice energy minimization results using the potential functions alone (see also Schröder and Sauer[28]). The reason for this

TABLE III.
Faujasite Structures Obtained for Di-Tetrahedra $(OH)_3SiOSi(OH)_3$ Models Embedded Using a Shell Model Potential.

O sites	O1	O2	O3	O4	Unit cell parameters
Embedded					
Cluster 1	**1.622**	1.616	1.635	1.624	17.42,
	137.2	156.1	150.1	145.4	60.0[a]
Cluster 2	1.633	**1.608**	1.629	1.623	
	139.5	**155.3**	150.1	144.4	
Cluster 3	1.634	1.618	**1.622**	1.623	
	139.9	153.7	**149.4**	144.7	
Cluster 4	1.635	1.618	1.633	**1.612**	
	140.2	153.9	149.7	**142.8**	
Fixed					
Cluster 1	**1.632**	1.617	1.609	1.616	—
	138.4	154.2	151.5	144.6	
Cluster 2	1.625	**1.619**	1.594	1.619	
	140.5	**155.3**	151.5	144.2	
Cluster 3	1.629	1.600	**1.616**	1.633	
	140.1	153.9	**148.5**	144.2	
Cluster 4	1.613	1.609	1.604	1.635	
	140.1	153.5	151.9	**145.0**	
Potential[b]	1.625	1.609	1.618	1.615	17.42
	140.5	154.2	151.7	144.7	60.0
Observed[c]	1.629	1.597	1.604	1.614	17.15
	140.1	149.3	145.8	141.4	60.0

Upper row, Si—O bond distances, in angstroms; lower row, Si—O—Si bond angles, in degrees.
[a] The cell parameters are not optimized.
[b] Ref. 28.
[c] Ref. 34.

might be the Taylor series expansion form of the force field. It requires going to high orders if an internal coordinate varies over a wide range of values, as is the case for zeolites and silicates.[15] The other possible reason is that a force field is not well suited for systems with ionic character, because adding point charge terms to a Taylor series expansion of the potential energy surface (which covers all interactions) may introduce linear dependencies. From Table III it is also seen that the restricted optimizations with the terminal hydroxyl groups fixed reflect the structure of faujasite. The angles are in good agreement with the experimental values, but all Si—O distances are too large.

Sodalite

The all-silica sodalite has high symmetry ($Im\bar{3}m$) and is therefore accessible for periodic HF benchmark calculations. The unit cell consists of a so-called cuboctahedron, which is built from four- and six-membered rings. This cuboctahedron can also be crosslinked in different manners to form other zeolite framework structures, such as faujasite and zeolite A. A di-tetrahedra model [T, T], a four-membered ring [R−T_4], and a spiro[3, 3] model in which two four-membered rings share one TO_4 tetrahedron are chosen as cluster models (Fig. 4). Table IV shows the optimized structures. They are directly comparable because the same basis sets and computational method [HF, DZP/TZP(O) basis set] were used in all the calculations, including the periodic *ab initio* calculations[27] and those for parameterizing the shell model potential. All of the performed embedded cluster calculations reproduce the structure of the periodic crystal. With increasing cluster size a better match of the results of the mechanical embedding calculations with the values obtained by periodic HF calculations is attained. Free-space optimizations of small- and medium-sized clusters are not able to reproduce the structures of specific polymorphs. Even a very large cluster comprising a full sodalite cage,[32] which is a large model and expected to be much more representative of the bulk, has a lower symmetry than the infinite solid. The optimization provides two different Si—O bond lengths and Si—O—Si bond angles even if the highest possible point group symmetry (O_h) is assumed. One of the Si—O bonds is part of two six-membered rings (labeled 6-6) and occurs twice, the other Si—O bond occurs only once and belongs to both a six- and a four-membered ring. The individual

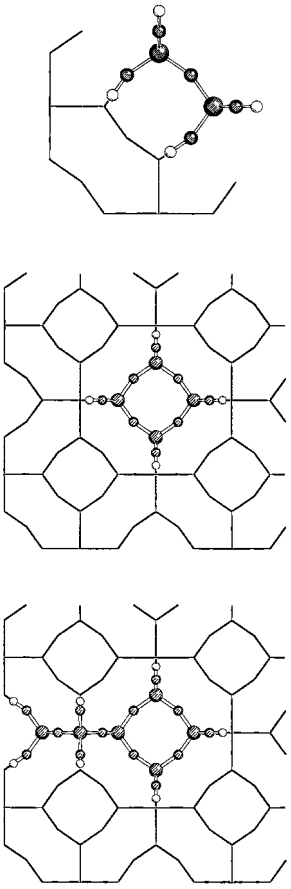

FIGURE 4. Cluster models used for sodalite. Top: di-tetrahedra model [T, T]; middle: four-ring model [R−T_4]; bottom: two spiro-connected four-rings models, spiro[3, 3].

values of the bond lengths and angles show larger deviations than those obtained with the embedding techniques. Nevertheless, the average values of the calculated bond distances and angles fit well with the results of the periodic HF calculation. It should also be noted that the structure predicted by the fitted potential alone agrees better with the experimental one than even with the periodic HF-optimized structure. This is probably caused by an error cancellation between the fitting error, the error due to neglect of electron correlation, and the fact that the observed structure refers to a sodalite containing ethylene glycol. The Si—O distances obtained by calculations with fixed coordinates of the boundary atoms are larger than those obtained with the embedding calculations.

α-Quartz

Two embedded cluster calculations were performed. A di-tetrahedra model [T, T] and a model

TABLE IV.
Optimized Sodalite Structures (Shell Model Potential Used for Embedding).

	r (Si—O) [Å]	∠(Si—O—Si) [deg]	Unit cell parameters[a]
Potential[b]	1.606	160.2	8.95
[T, T] $(OH)_3SiOSi(OH)_3$			
Embedded	1.607	161.5	8.95[e]
Fixed	1.615	160.3	—
[R –T_4] $Si_4O_4(OH)_8$			
Embedded	1.608	160.8	8.95[e,f]
Fixed	1.617	161.6	—
Spiro[3, 3] $Si_7O_8(OH)_{12}$			
Embedded	1.608	160.7	8.95[e,g]
Fixed	1.613	161.4	—
Free sodalite cage			
(4-6)	1.615	162.0	8.97
(6-6)	1.605	158.2	
Weighted average	1.612	160.7	
Crystal[c]	1.612	160.6	8.99, 8.99, 8.99
Observed[d]	1.586(1)	159.6(1)	8.83, 8.83, 8.83

[a] All angles 90.0°. [b] Ref. 28. [c] Ref. 27. [d] Ref. 35; the cage of the sodalite structure investigated contains ethylene glycol. [e] The cell parameters are not optimized. [f] Unit cell size 17.90 × 17.90 × 8.95 was used. [g] Unit cell size 17.90 × 17.90 × 17.90 was used.

which contains three complete coordination spheres about a central Si atom (shell-3) [TT_4] (Fig. 5) were chosen as cluster models. α-quartz has two different Si—O bond lengths. All calculations including the lattice energy minimization with the shell model potential reproduce this feature. The absolute values of the Si—O bond lengths and Si—O—Si bond angles are in good agreement with the experiment. The differences between the two Si—O bond distances improves compared with the lattice energy minimization results when *ab initio* corrections are made by the embedding approach. The improvement follows the size of the embedded cluster. A possible explanation for this is that the error cancelation due to eqs. (10) and (11) is better the larger the cluster is. Despite the high symmetry of α-quartz (space group $P3_121$) periodic HF calculations with the present basis set are not available. They are more demanding than for sodalite, because of the dense structure of α-quartz. As for other systems the restricted optimization yields too-large Si—O distances. The difference between the two Si—O bond lengths is much too small and almost disappears when the cluster size is increased.

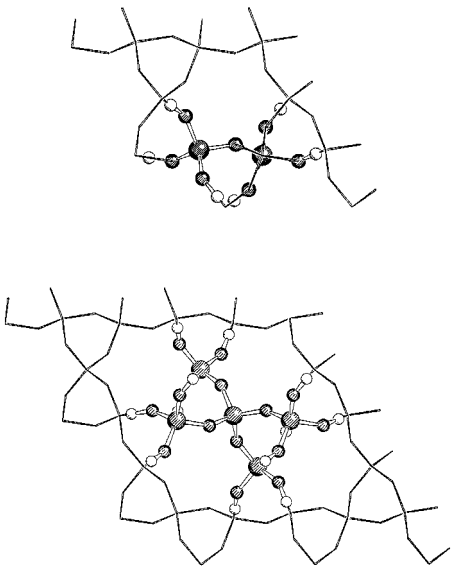

FIGURE 5. Cluster models used for α-quartz. Top: di-tetrahedra model [T, T]; bottom: shell 3 model [TT_4]. There are no closed rings in the shell 3 model. Some atoms are hidden due to the projection used.

Comparison of Different Polymorphs

It is also interesting to compare the results of the embedding cluster calculations for different framework structures and to look for the minimum cluster size that is necessary to model the structural differences between different polymorphs. For this purpose, results for the embedded di-tetrahedra and also for embedded monotetrahedron models are listed in comparison to

TABLE V.
Optimized α-Quartz Structures (Shell Model Potential Used for Embedding).

	r (Si—O)/Δr (Si—O) [Å]	∠(Si—O—Si) [deg]	Unit cell parameters
Potential[a]	1.614/0.003 1.617	148	4.99, 4.99, 5.51, 90.0, 90.0, 120.0
[T, T] $(OH)_3SiOSi(OH)_3$			
Embedded	1.612/0.007 1.619	147	9.98, 9.98, 11.01, 90.0, 90.0, 120.0[b]
Fixed	1.621/0.004 1.625	148	—
[T−T_4] $Si_5O_4(OH)_{12}$			
Embedded	1.610/0.008 1.618	148	14.96, 14.96, 16.52, 90.0, 90.0, 120.0[b]
Fixed	1.618/0.001 1.619	148	—
Observed[c]	1.605/0.009 1.614	144	4.92, 4.92, 5.41, 90.0, 90.0, 120.0

[a] Ref. 28. [b] The cell parameters are not optimized. [c] Ref. 36.

results for the free-space optimized models (Table VI). For the di-tetrahedra model the constraint of a mirror plane is needed (C_s symmetry)[32] to avoid the formation of intramolecular hydrogen bridges, which would lead to an unrealistic distortion of the configuration. It is not possible to define larger models which are identical for all polymorphs. For example, it is not possible to choose a four-membered ring as a cluster model for quartz, but it is also not possible to find a shell 3 model for faujasite which does not have closed rings. This limits the comparability beyond di-tetrahedra models. Tables IV and V show that bond distances and angles are almost converged if di-tetrahedra models are chosen. The influence of the framework is evident even if a one-tetrahedron model is embedded, which is the smallest possible one. The Si—O bond in sodalite is found shorter than in quartz for both cluster models. The trend of the Si—O—Si angle values is also described properly. This shows that, using the embedding technique, even small clusters can model the differences in the local structure of different silica polymorphs.

Conclusions

A method was presented which combines the HF method with potential function calculations to

TABLE VI.
Influence of Embedding Framework on Structure Predictions.

	Sodalite	Quartz	Free molecule
[T]	1.619	1.625, 1.631	1.626
$Si(OH)_4$	160	147	119
[T, T]	1.607	1.612, 1.619	1.610
$(OH)_3SiOSi(OH)_3$	162	148	180
Observed	1.586(1)[a] 159.6(1)	1.605; 1.614[b] 144	—

Upper row, Si—O bond distances, in angstroms; lower row, Si—O—Si bond angles, in degrees.
[a] Ref. 35. [b] Ref. 36.

describe periodic structures. This method is easily extended to other computational methods such as density functional theory or MP2 perturbation theory. Application to silica polymorphs shows that this combination scheme leads to an improvement over the results obtained by potential functions alone. The structures of the cluster are influenced by the framework structure. The inner parts of the cluster are better described than the outer ones.

The convergence of the structure with respect to the cluster size is much stronger than for free-cluster calculations. The calculated energies of clusters with different crystallographic positions, but the same size, are comparable in contrast to calculations of molecules with fixed coordinates. The calculated energies of clusters of the same size are comparable for a given polymorph, even if they model different crystallographic sites. This makes the method suitable to study energy differences for processes like isomorphous substitution of, e.g., (Al, H) or Ti, into different crystallographic Si sites. In contrast, the energies obtained for cluster models with fixed nuclear coordinates are not comparable.

Acknowledgments

A substantial share of this work has been done within Biosym/MSI's Catalysis and Sorption Project. The Catalysis and Sorption Project is supported by a consortium of industrial, government, and academic institutions. The stimulating atmosphere within the Catalysis and Sorption team was greatly beneficial for this project. We thank K.-P. Schröder and M. Brändle for providing unpublished results as well as R. Ahlrichs (Karlsruhe) and J. Gale (London) for making available recent versions of the TURBOMOLE and GULP codes, respectively.

References

1. J. Gao, In *Reviews in Computational Chemistry*, *Vol. 7*, K. B. Lipkowitz and D. B. Boyd, Eds., VCH, New York, 1995, p. 119.
2. D. Bakowies and W. Thiel, *J. Phys. Chem.*, **100**, 10580 (1996).
3. T. Matsubara, F. Maseras, N. Koga, and K. Morokuma, *J. Phys. Chem.*, **100**, 2573 (1996).
4. U. C. Singh and P. A. Kollman, *J. Comput. Chem.*, **7**, 718 (1986).
5. M. J. Field, P. A. Bash, and M. Karplus, *J. Comput. Chem.*, **11**, 700 (1990).
6. R. V. Stanton, D. S. Hartsough, and K. M. Merz, Jr., *J. Phys. Chem.*, **97**, 11868 (1993).
7. R. V. Stanton, D. S. Hartsough and K. M. Merz, Jr., *J. Comput. Chem.*, **16**, 113 (1995).
8. F. Maseras and K. Morokuma, *J. Comput. Chem.*, **16**, 1170 (1995).
9. A. Warshel, *Computer Modelling of Chemical Reactions in Enzymes and Solutions*, Wiley, New York, 1991.
10. J. Sauer, In *Zeolites and Related Microporous Materials: State of the Art 1994. Studies in Surface Science and Catalysis*, *Vol. 84*, J. Weitkamp, H. G. Karge, H. Pfeifer, and W. Hölderich, Eds., Elsevier, Amsterdam, 1994, p. 2039.
11. J. Sauer, *Chem. Rev.*, **89**, 199 (1989).
12. J. Sauer, J.-R. Hill, U. Eichler, and C. M. Kölmel, Abstracts of the International Workshop on Electronic Structure Methods for Truly Large Systems, August 1–7, 1994, Braunlage (Harz), Germany.
13. SOLIDS_EMBED Program, Version 1.0 in Catalysis Release 3.0: Biosym Technologies, Inc., San Diego, CA 1993.
14. U. Eichler, Ph.D. thesis, Humboldt-Universität zu Berlin (in preparation).
15. J.-R. Hill and J. Sauer, *J. Phys. Chem.*, **99**, 9536 (1995).
16. S. J. Weiner, P. A. Kollman, D. A. Case, U. C. Singh, C. Ghio, G. Alagona, S. Profeta, Jr., and P. Weiner, *J. Am. Chem. Soc.*, **106**, 765 (1984).
17. B. R. Gelin and M. Karplus, *Biochemistry*, **18**, 1256 (1979).
18. U. Burkert and N. L. Allinger, *Molecular Mechanics*, ACS, Washington, DC, 1982.
19. P. Dauber-Osguthorpe, V. A. Roberts, D. J. Osguthorpe, J. Wolff, M. Genest, and A. T. Hagler, *Prot. Struct. Funct., Genet.*, **4**, 31 (1988).
20. J. R. Maple, U. Dinur and A. T. Hagler, *Proc. Nat. Acad. Sci. USA*, **85**, 5350 (1989).
21. DISCOVER Program, Biosym/MSI, San Diego, CA, 1992.
22. B. G. Dick and A. W. Overhauser, *Phys. Rev.*, **112**, 90 (1958).
23. GULP Program (the General Utility Lattice Program), written and developed by J. D. Gale, Royal Institution/Imperial College, UK, 1992–1994.
24. TURBOMOLE Program, R. Ahlrichs, M. Bär, M. Häser, H. Horn, and C. Kölmel, *Chem. Phys. Lett.*, **162**, 165 (1989). TURBOMOLE is commercially available from MSI, San Diego, CA.
25. DMOL Program, B. Delley, *J. Chem. Phys.*, **92**, 508 (1990). DMOL is commercially available from MSI, San Diego, CA.
26. (a) MOPAC Program, J. J. P. Steward, MOPAC 6.0 QCPE, Program No. 455; (b) M. J. S. Dewar and W. Thiel, *J. Am. Chem. Soc.*, **99**, 4899 (1977). (c) M. J. S. Dewar, E. G. Zoebisch, E. F. Healy, and J. J. P. Stewart, *J. Am. Chem. Soc.*, **107**, 3902 (1985).
27. M. Brändle and J. Sauer (unpublished results).
28. K.-P. Schröder and J. Sauer, *J. Phys. Chem.*, **100**, 11043 (1996).
29. J. Sauer, H. Horn, M. Häser, and R. Ahlrichs, *Chem. Phys. Lett.*, **173**, 26 (1990).

30. S. Huzinaga, *Approximate Atomic Wavefunctions I, II*. University of Alberta, Edmonton, Alberta, Canada, 1971.
31. S. Huzinaga, *J. Chem. Phys.*, **42**, 1293 (1965).
32. J.-R. Hill and J. Sauer, *J. Phys. Chem.*, **98**, 1238 (1994).
33. A. Schäfer, H. Horn, and R. Ahlrichs, *J. Chem. Phys.*, **97**, 2571 (1992).
34. J. A. Hriljac, M. M. Eddy, A. K. Cheetham, J. A. Donohue, and G. J. Ray, *J. Solid State Chem.*, **106**, 66 (1993).
35. J. W. Richardson, Jr., J. J. Pluth, J. V. Smith, W. J. Dytrych, and D. M. Bibby, *J. Phys. Chem.*, **92**, 243 (1988).
36. L. Levien, C. T. Previtt, and D. J. Weidner, *Am. Mineral*, **65**, 920 (1980).